

UC Riverside

UC Riverside Previously Published Works

Title

Effect of LED Light Frequency on an Object in Terms of Visual Comfort

Permalink

<https://escholarship.org/uc/item/24g8p1gs>

Journal

Electric Power Components and Systems, ahead-of-print(ahead-of-print)

ISSN

1532-5008

Authors

Ozcelik, Mehmet Ali

Akinci, Tahir Cetin

Yilmaz, Musa

et al.

Publication Date

2023-12-08

DOI

10.1080/15325008.2023.2281629

Copyright Information

This work is made available under the terms of a Creative Commons Attribution License, available at <https://creativecommons.org/licenses/by/4.0/>

Peer reviewed



Effect of LED Light Frequency on an Object in Terms of Visual Comfort

Mehmet Ali Ozcelik,¹ Tahir Cetin Akinci,^{2,3} Musa Yilmaz,^{4,5} and Alfredo A. Martinez-Morales⁴

¹Technical Science Department Electrical and Energy, Gaziantep University, Şehitkamil - Gaziantep, Türkiye

²Electrical Engineering, Istanbul Technical University, Sarıyer, Istanbul, Türkiye

³WCGEC, University of California Riverside, CA, USA

⁴CE-CERT, University of California Riverside, CA, USA

⁵Electrical and Electronics Engineering, Batman University, Batman, Türkiye

CONTENTS

- 1. Introduction
- 2. Experimental Setup
- 3. Results
- 4. Discussion
- 5. Conclusion
- References

Abstract—Light emitting diodes (LEDs) play an essential role in lighting, and green earth activities because of their high efficiency, longevity, and reduction of carbon dioxide emissions during illumination. However, the brightness level of LED light sources must be adjusted appropriately for the backlight source or illumination; therefore, pulse amplitude modulation (PWM) is a commonly used method of LED control. This article experimentally investigated human interaction with the visual comfort effect of the light obtained using different PWM frequencies on an object in a sensor-based intelligent lighting system. Critical light frequencies are vital for the eye to distinguish light stimuli according to time. Histograms of the object were created according to the light frequency, and the results are discussed. The eye's response to light frequencies changing over time is important for visual comfort, and examining light frequencies in the range of 25–250 Hz was sufficient to conclude the study. It has been experimentally shown that light frequencies around 160 Hz, and above this value provide visual comfort.

1. INTRODUCTION

Energy saving and efficiency, using green energy resources, and reducing carbon emissions are essential issues worldwide [1–4]. Lighting is vital to worldwide energy consumption in many ways [5]. Regarding energy consumption, lighting constitutes a significant amount of electricity produced in developing countries [6, 7]. More than 20% of the energy provided in developed countries is consumed by lighting [8]. Fluorescent lamps and incandescent filament lamps have been used in lighting devices [9–13], and these lamps are replaced by LEDs because of their long-term usability, high light effectiveness, and high performance [10, 14–17].

Keywords: LED, pulse width modulation (PWM), human interaction with light, histogram specification, flicker effect, visual comfort zone

Received 3 October 2023; accepted 1 November 2023

Address correspondence to Mehmet Ali Ozcelik, Gaziantep University, Technical Science Department Electrical & Energy, 27310 Şehitkamil - Gaziantep, Türkiye. E-mail: ozcelik@gantep.edu.tr

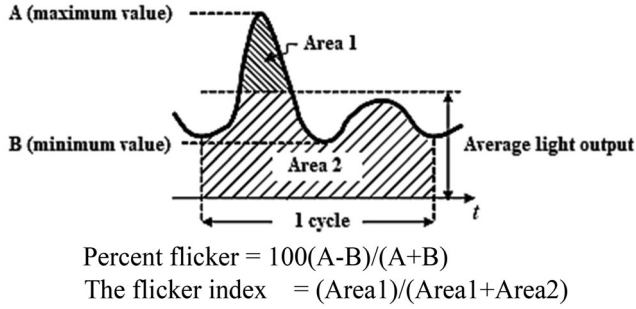


FIGURE 1. Definition of percentage flicker and flicker index [19].

LED light sources are used in driver circuits, and these drivers can cause visible flicker [18]. Flicker can be defined as an instantaneous change of light intensity in the light source. As seen in Figure 1, flicker can be measured using two parameters: percent flicker, and flicker-index. Percentage flicker can be defined as the ratio between the maximum, and minimum light in a cycle. In addition, the flicker index requires accurate measurement of the waveform shape with complex integral mathematics. For this reason, the expression percent flicker is used more than the flicker index to qualify the amount of flicker. Additionally, the IEEE PAR1789 standard specifies possible health risks associated with higher percentages of flicker [19, 20].

The human eye’s time-varying excitations can be distinguished in cases where light excitations change very slowly, as in natural lighting, and in cases where light excitations change very quickly, as in discharge lamps working with alternating current. If the brightness of the light source changes periodically, and this change appears to the eye as a steady glowing light source, this flicker frequency is critical. The mean value of the periodically changing luminance (L_{mean}) is calculated by Eq. (1), where L is the instantaneous value of the periodically changing luminance, and T is the period of the periodically changing luminosity.

$$L_{mean} = \frac{1}{T} \int_0^T L(t) dt \quad (1)$$

Studies to explore the effects of light illumination require a continuous approach to situations such as bright, and dim light conditions. Various studies have confirmed that the illumination of LED lights affects human attention, but there are no consistent research results as to what level of illumination is effective [21]. The Kruithof curve defines a region of lighting levels and color temperatures generally seen as comfortable or pleasant to an observer. This

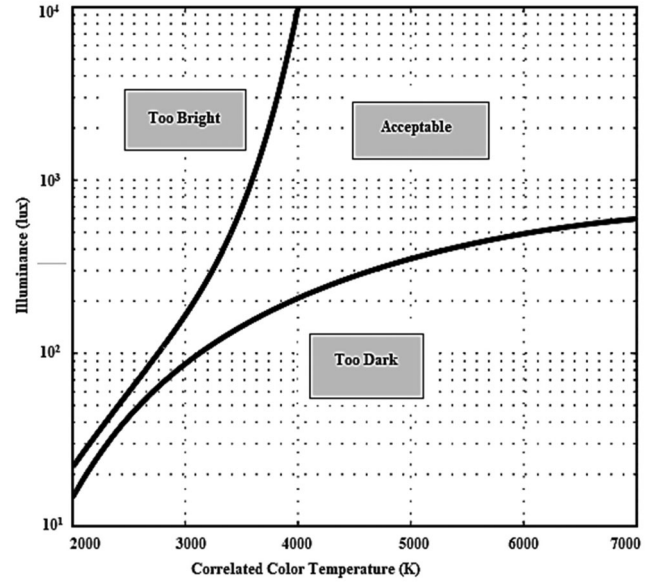


FIGURE 2. The Kruithof curve was used in this study as a criterion to capture the human comfort factor [22].

empirical curve captures the “comfortable” lighting range parameterized by brightness and color temperature, which is called the Kruithof curve [22]. It has been empirically determined that the Kruithof curve for a given value of L luminance and color temperature (K) is comfortable for humans; this curve is shown in Figure 2.

Luminous efficiency (LE) can be defined as the ability of a light source to efficiently produce visible light output and is measured in lumens per Watt. The high performance and efficiency of LEDs play an important role in their preference. In the simulations reported, the LER (luminous efficiency of radiation) of each LED mixture can be quoted, which should be as high as possible to ensure a modern, energy-efficient lighting design. LER is defined by the lighting efficiency equation (2), and the overall lighting efficiency (LE) is defined by Eq. (3), [23].

$$LER = \frac{K_m \int_{\lambda}^0 V(\lambda) S(\lambda) d\lambda}{\int S(\lambda) d\lambda} \quad (2)$$

$$LE = \frac{K_m \int_{\lambda}^0 V(\lambda) S(\lambda) d\lambda}{P_E} \quad (3)$$

where K_m is the maximum luminous efficiency of radiation (≈ 683 lumens/watt), S_{λ} is the spectral distribution of the light source, and V_{λ} is the CIE spectral sensitivity function value for human photonic vision. Therefore, LER evaluates the “illumination content” of the spectrum by

comparing the visible light lumen output to the total radiant watt. LE, on the contrary, is the electricity consumption (PE) that must cover the transformation losses in the illumination source, and the total-radiant output, as shown in (4).

$$P_E = C_L + \int S_\lambda d_\lambda \quad (4)$$

here CL symbolizes the conversion losses due to the physical process of the lamp. The portion in formula (2) is always greater than that in formula (1), so LE is always less than LER. Moreover, LER is easier to guess because it depends only on the spectrum source of illumination.

PWM is a type of modulation that adjusts brightness by quickly turning the light source on and off. Frequency and duty cycle are essential parameters in PWM [24]. The period equals the sum of the T_{ON} time and the T_{OFF} time. The frequency (F) of a PWM signal is found in $1/\text{period}$. The PWM signal is shown in Figure 3, and the duty cycle expression is given by Eq. (5).

$$\text{duty cycle}(D) = \frac{T_{ON}}{T_{ON} + T_{OFF}} 100 \quad (5)$$

Image processing is a method used to obtain a specific image by converting it into a digital form or to obtain the desired result from the image with software. Today, image processing is used in many fields, such as medicine, military, security, facial recognition, emotion analysis, robotics, and classification. Histograms allow us to see the frequency distribution of the dataset as, a graphical representation of the image gray value distribution. For example, as you move to the left on the X-axis (closer to the origin), pixels of darker and black areas are obtained [25, 26].

In this study, the visual comfort effect of light on a vase object was experimentally investigated using different PWM frequencies in an intelligent lighting system using a

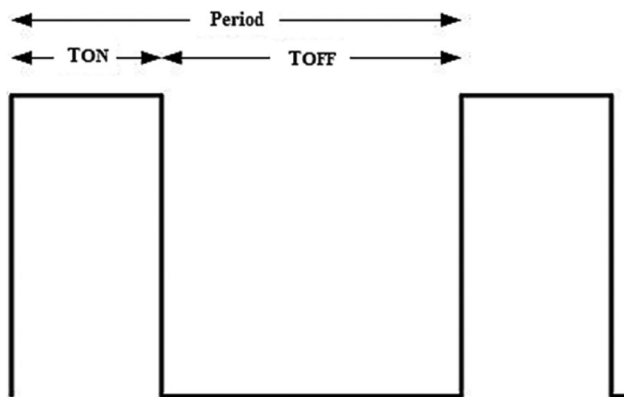


FIGURE 3. PWM signal.

phototransistor sensor. The reference illuminance of the environment was adjusted to 300 lux using a potentiometer, and LED panels were used to obtain the required illuminance level. According to the light frequency, the histograms of the object were created in the MATLAB software environment and, interpreted.

2. EXPERIMENTAL SETUP

The power of the LED panel used was 36 W, the maximum luminous flux value was 3204 Lumens, the color temperature was 6500 K, and the luminous factor was 89 lm/W. An LED panel with a color rendering index (CRI) >80 is used. The light distribution curve of the LED panel is shown in Figure 4. Based on the EN 12464 lighting of indoor workplaces standard, the recommended classroom light level is 300 lux [28]. The color temperature of the LED panel was maintained at 6500 K, and the illumination in the environment was 300 lux. Considering these values, the Kruithof curve in Figure 2 shows that the light values are acceptable; and in the comfort zone.

A TEMT6000 phototransistor light sensor was used in this study [29]. This sensor can measure illuminance up to 1000 lux with peak sensitivity of approximately 580 nm, with a spectral sensitivity curve adapted to suit human eye sensitivity. The photo sensor generates analog current information from a variable voltage of 0–5 V read through

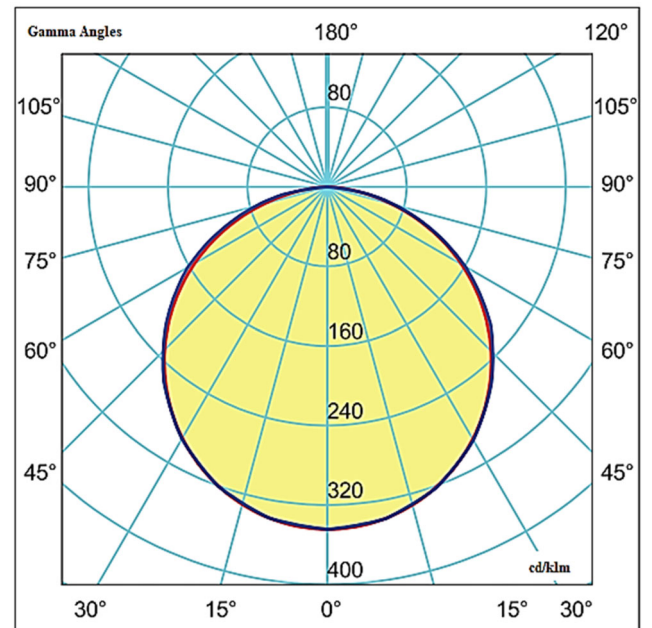


FIGURE 4. Light distribution curve of the LED panel [27].

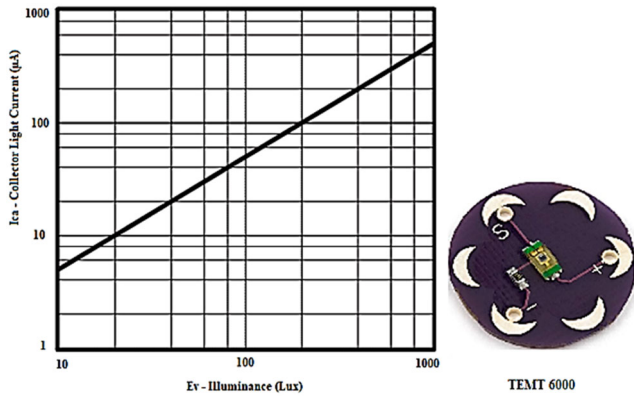


FIGURE 5. Collector light current and illuminance of the TEMT 6000 [29].

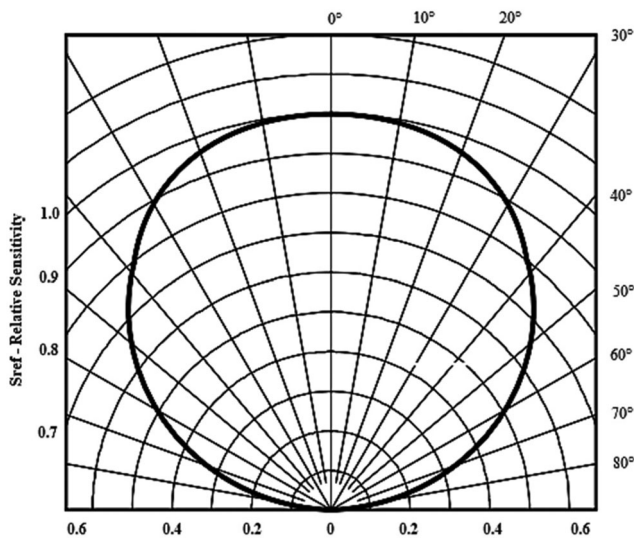


FIGURE 6. Relative radiant sensitivity vs. angular displacement of the TEMT 6000 [29].

a 10K resistor. The current change of the sensor with brightness is shown in Figure 5.

The TEMT6000 sensor has an angle accuracy of $\phi = \pm 60^\circ$. The relative radiation sensitivity, and angular displacement are given in Figure 6. This photo sensor is strictly linear between ≤ 10 and ≥ 1000 luxes, and its typical photocurrent is specified for $50 \mu\text{A}$ (at 100 lx). The photocurrent (I_{PCE}) illumination formula of the light sensor is given below.

$$\text{Illuminance (lux)} = \frac{1}{2} I_{PCE} (\mu\text{A}) \quad (6)$$

The reference illumination level can be adjusted with a 10 K potentiometer connected to the ambient lighting sensor. The reference value was set at 300 lux. The light is increased if the analog information received from the

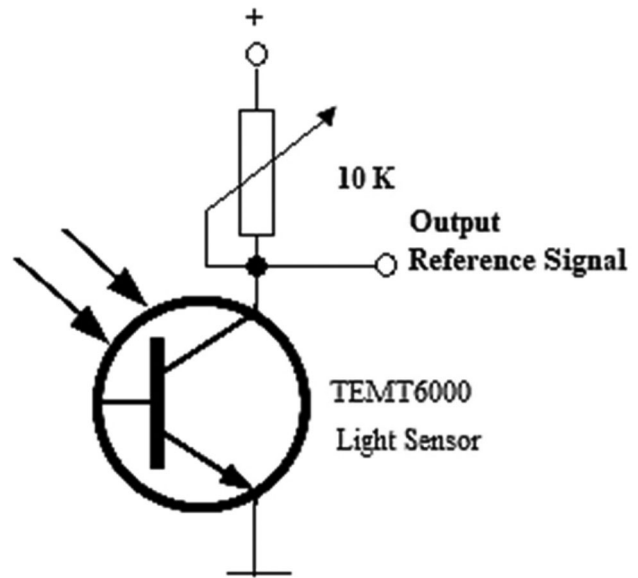


FIGURE 7. Generation of the reference signal.

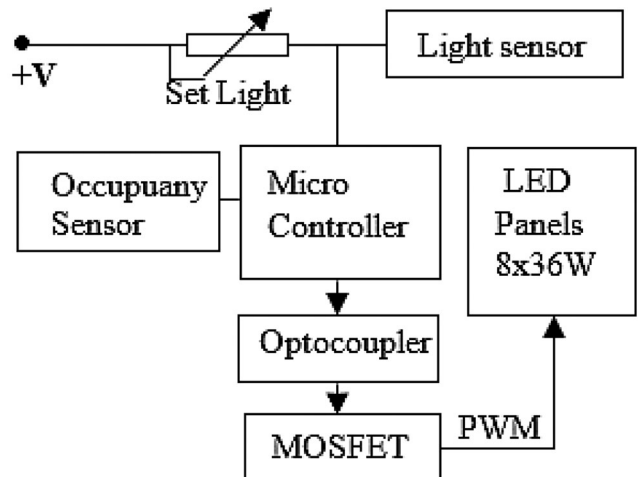


FIGURE 8. Lighting system structure.

phototransistor light sensor is below the reference value. Figure 7 shows the reference signal generation for indoor illumination.

In the smart LED lighting system, the ambient reference value can be obtained, and connected to the TEMT6000 ambient light sensor so that the potentiometer adjusts the block graph shown in Figure 8. The reference value was set to 300 lux. If the light information received from the ambient sensor is lower than the reference lux limit, the amount of light increases.

Increasing or decreasing the ambient light is accomplished with the PWM signal generated by the algorithm shown in Figure 9. The PWM signal produced by the

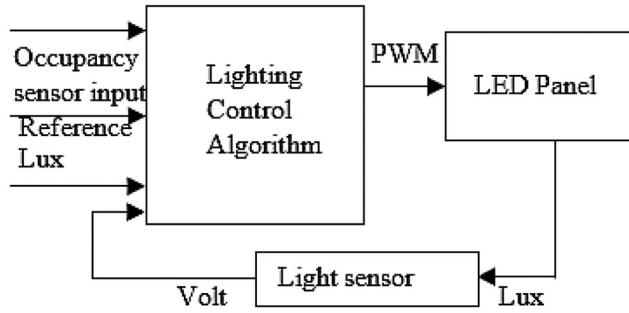


FIGURE 9. Control algorithm PWM frequency of the LED lighting system.



FIGURE 10. Experimental environment.

control card determines the light level at which the LED panels pass through the MOSFET transistor.

In the experimental setup, a colored flower vase was used as the object. The distance between the flower vase and the ceiling was 1.1 m. The ceiling and walls are light in color. The image of the experimental environment is shown in Figure 10.

3. RESULTS

Experimental measurements were conducted with light frequencies of 25, 50, 125, 166, and 250 Hz. These images were taken between 0, and 4. Seconds at each PWM light frequency. All images were obtained from the camera recording with a resolution value of 720. The average pixel value of each picture is shown with a red line and is given as numerical values in the figure tag. In the histograms, the Y-axis indicates the number of pixels, and the X-axis shows the brightness value between 0 and 255 obtained using 8 bits. The histograms show how illuminated each pixel is. The left side of the X-axis represents pure black,

and the right side represents brightness with pure white. The number of pixels of the relevant brightness value on the Y-axis is shown numerically.

3.1. Case 1

In the video recording taken at 25 Hz light frequency, the histogram pixel values of the image vary considerably with time. In Figure 11, the red line shows the average of the pixels in the image histogram. The origin point on the X-axis shows the dark level. As it moves from the origin point to the left of the X-axis, the image brightness in light color increases.

While the pixel average of the images taken at 25 Hz between 0 and 1 s is 77.2523, the standard in seconds is 122.1436. When watching the video recording of the pictures, the flicker effect caused by the pixel changes according to time disrupted the visual comfort. The average of the five values is 88.6269

3.2. Case 2

In the video recording taken at 50 Hz light frequency, the histogram pixel values of the image vary considerably according to time. Figure 12 shows the average pixel values of the pictures taken from the images recorded between 0, and 4 s. For example, while the average pixel value of the image between 0, and 1 is 94.0241, the average pixel at the third second is 165.9061

When viewing a video recording of images at 50 Hz, the flicker effect caused by the pixel changes according to the time period disrupted visual comfort. The average of the five values is 113.387.

3.3. Case 3

In the video recording taken at 125 Hz light frequency, the histogram pixel values of the image vary considerably with time. Figure 13 shows the average pixel values of the pictures taken from the image recorded between 0 and 4 seconds. For example, while the average pixel value of the image between 0 and the 1st second is 72.3844, the average pixel value in the 1st second is 152.4702.

The flicker effect caused by the pixel changes according to the time when watching the video recording of the images at 125 Hz disrupted visual comfort. The average of the five values is 108.255

3.4. Case 4

The histogram pixel values of the image in the video recording taken at a light frequency of 166 Hz do not

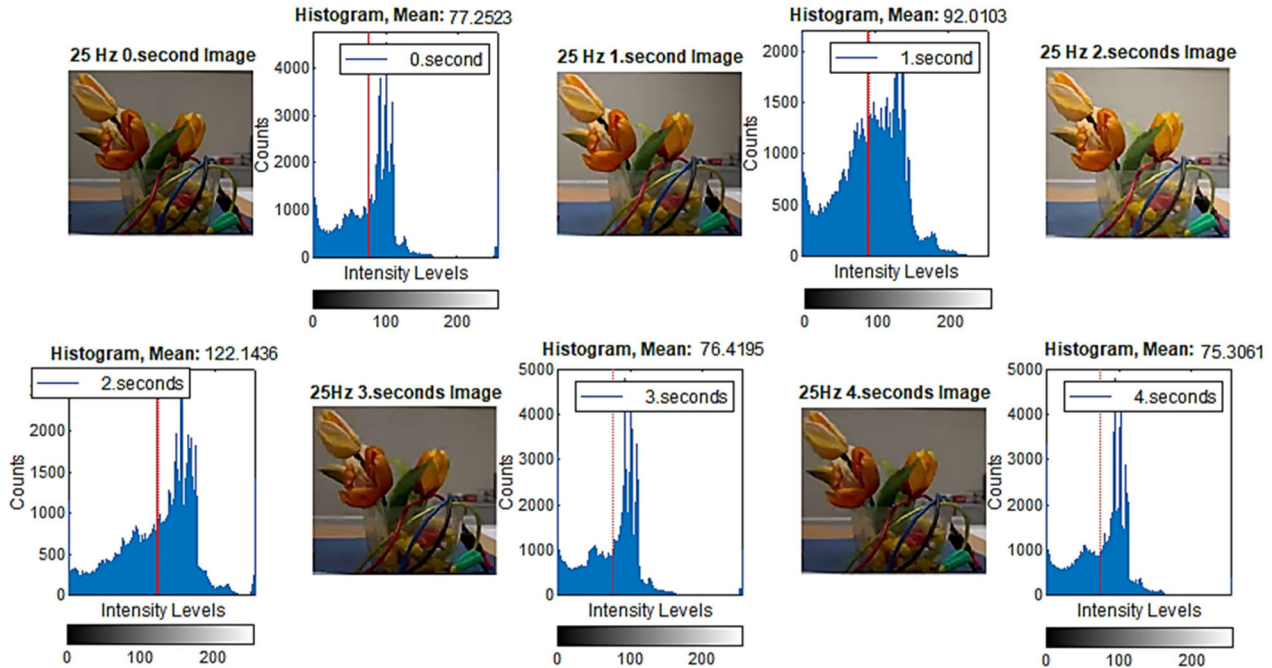


FIGURE 11. Average histogram values of the image according to the time range at 25 Hz light frequency, period 0.04 s.

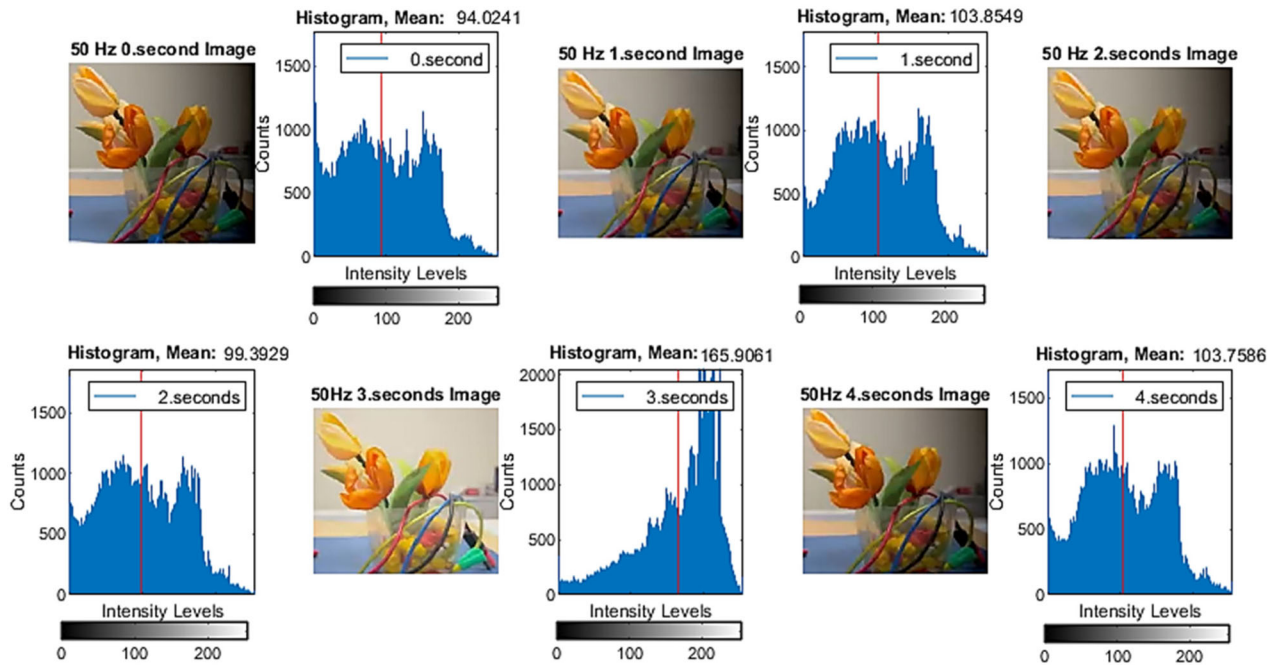


FIGURE 12. Average histogram values of the image according to the time range at 50 Hz light frequency, period 0.02 s.

change with time. Therefore, these values can be considered constant when the video recording is watched or compared with the picture. Figure 14 shows the average pixel values of the photographs taken from the image

recorded between 0 and 4 s. The average pixel value of the image is between 0. The second and first second is 120.838, while the average pixel value at the second is 121.1245

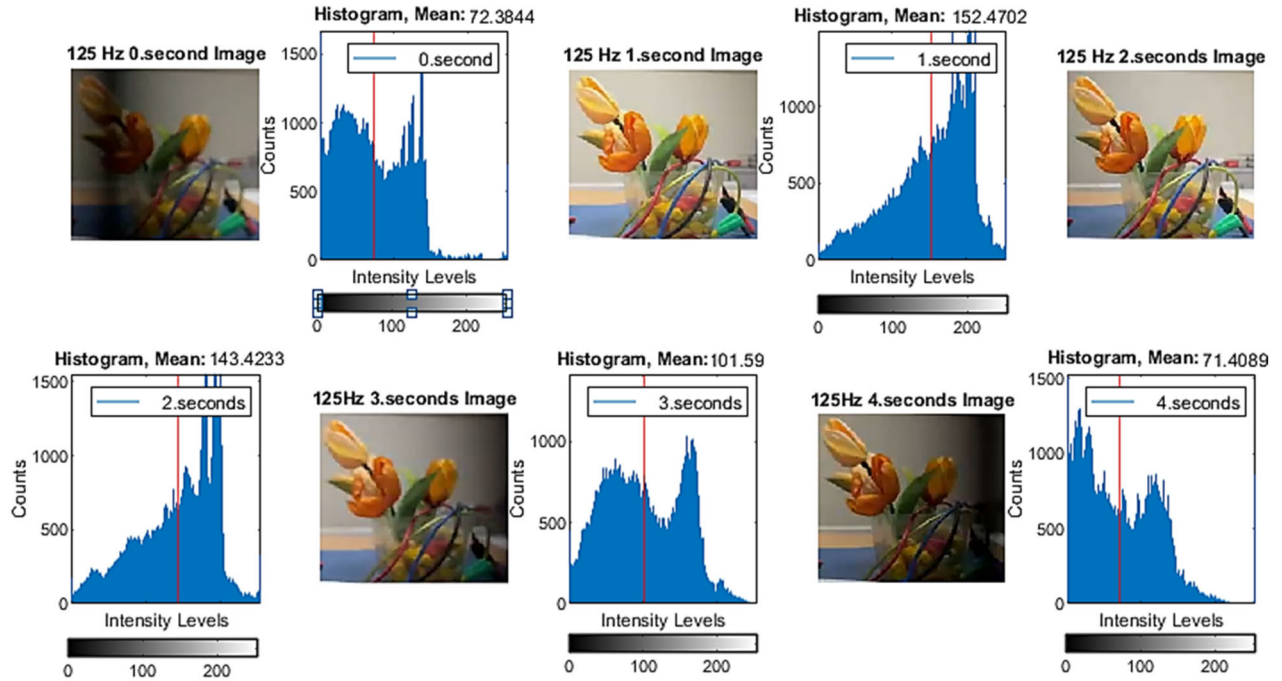


FIGURE 13. Average histogram values of the image over the time range at 125 Hz light frequency, period 0.008 s.

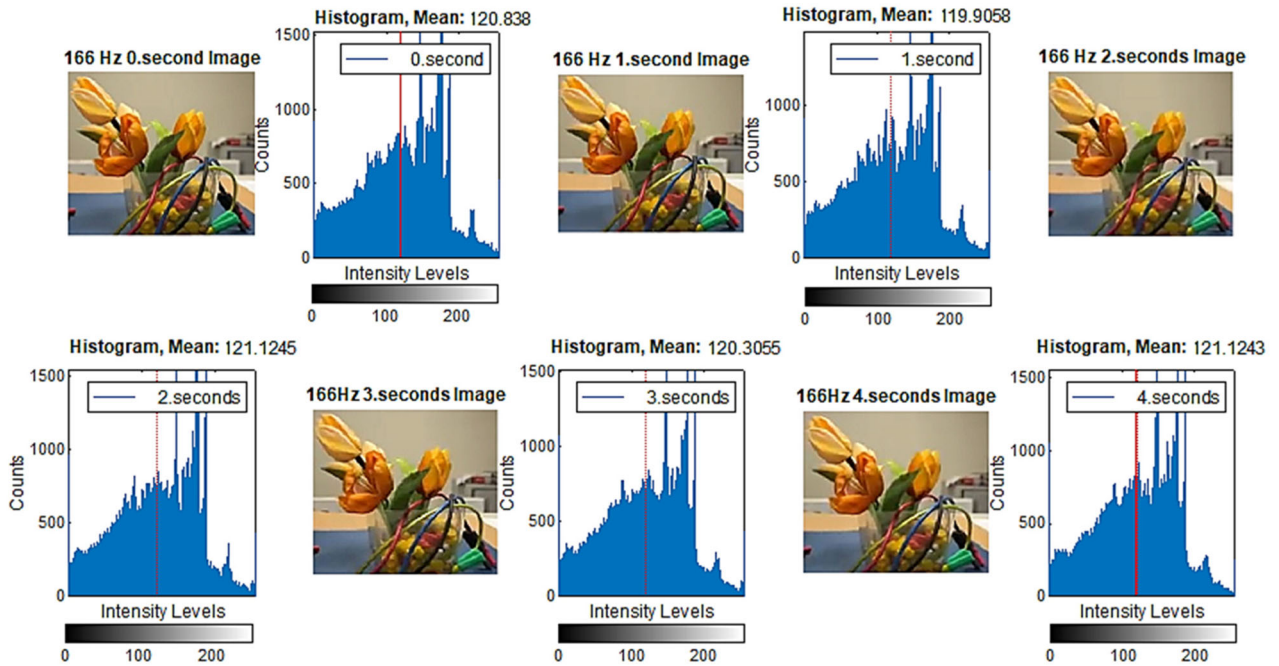


FIGURE 14. Average histogram values of the image over the time range at a light frequency of 166 Hz, period of 0.006 s.

When the video recording of the images was watched at 166 Hz, the flicker/frequency effect caused by the time change of the pixels could not be noticed, and it was observed that visual comfort was created. The average of the five values is 120.6596.

3.5. Case 5

In the video recording shot at a light frequency of 250 Hz, the histogram pixel values of the image almost do not change over time. Therefore, these values can be considered constant when watching the video recording or

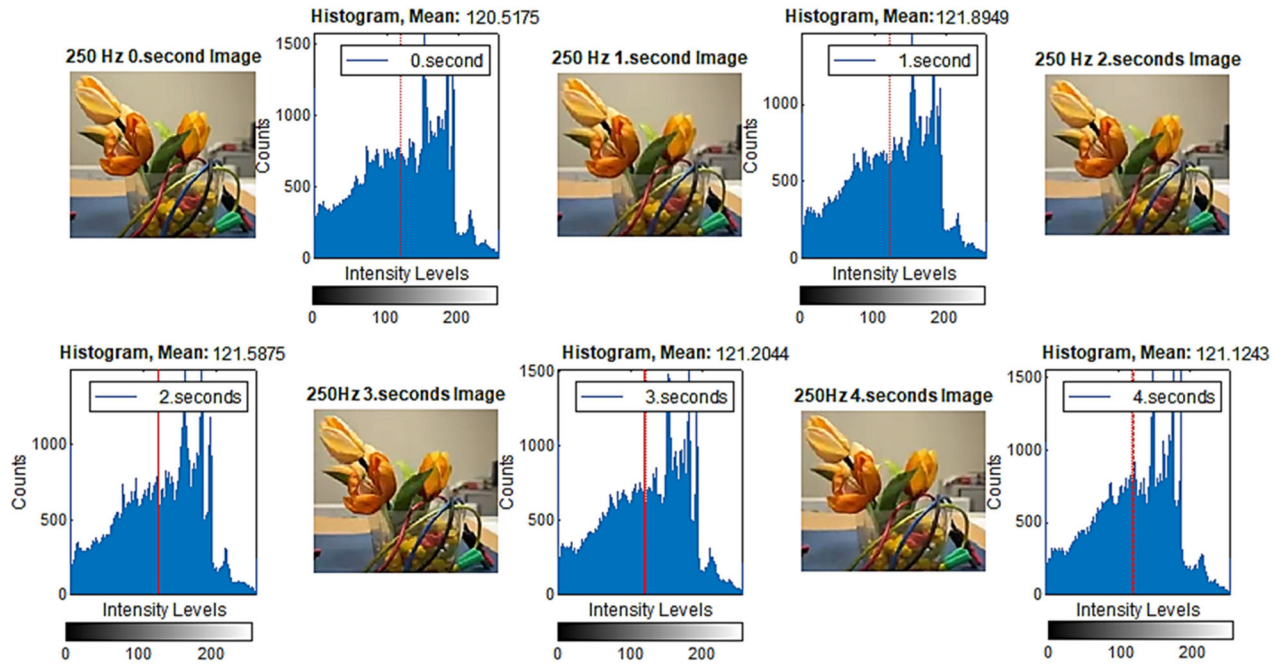


FIGURE 15. Average histogram values of the image over the time range at 250 Hz light frequency, period 0.004 s.

Time	25 Hz	50 Hz	125 Hz	166 Hz	250 Hz
0 second	77.2523	94.0241	72.3844	120.838	120.5175
1 second	92.0103	103.8549	152.4702	119.9058	121.8949
2 seconds	122.1436	99.3929	143.4233	121.1245	121.5875
3 seconds	76.4195	165.9061	101.59	120.3055	121.2044
4 seconds	75.3061	103.7586	71.4089	121.1243	121.1243
MEAN	88.62636	113.3873	108.2554	120.6596	121.2657
STD	19.94155	29.63351	38.34237	0.537937	0.520337

TABLE 1. Average (mean), and STD values of light frequencies over a time range.

examining the pictures. Figure 15 shows the average pixel values of the images taken from the image recorded between 0 and 4 s. For example, the average pixel value of the image between the 0th and, 1st seconds is 120.5175, while the average pixel value at the 1st second is 121.8949.

When watching the video recording of the images at 250 Hz, the flicker effect caused by the pixel changes with time was not observed, and visual comfort was provided. The average of five values is 121.2657.

4. DISCUSSION

When the standard deviation values of the frequencies were examined according to Table 1, significant standard

deviation (STD) values were obtained at 25, 50, and 125 Hz light frequencies, and minimal STD values were obtained at 166 and 250 Hz.

In Table 1, whether there is a flicker according to time in the vase object image in the camera kept fixed under a specific light frequency has been observed. The visual comfort status of these flickers was determined from the average pixel values of the images taken in at particular seconds. The average pixel value of the image remained constant over time, or the low standard deviation value was used to measure image quality. In Figure 16, the average, and STD changes of the light frequencies are shown. At 166, and 250 Hz, the STD values are lower, and the pixel density is relatively higher.

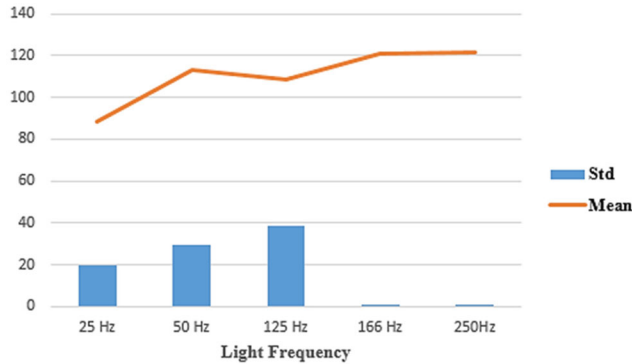


FIGURE 16. Average and STD values of the light frequencies.

5. CONCLUSION

CRI, and color-temperature (Kelvin) are essential for visual comfort. The scale range of the color-rendering index is between 0, and 100. Natural-lighting has a CRI of 100, and a CRI greater than 80 is recommended. The color-rendering index of the LED lamps chosen for illuminating the space, and the color temperature are greater than 80. The color temperature of the LED panel used was 6500K. The region where the 300-lux reference value provided by intelligent lighting, according to the Kruithof curve and the color temperature of the LED lamp intersect, is located in the visual comfort zone.

In this research, color temperature and lux brightness values are discussed in terms of human visual comfort, and fluctuations. The histogram technique and diagrams are effective in showing the visual comfort of the light frequency effect. The high flicker effect in images taken from 25, 50, and 125 Hz light frequencies according to time has been shown with high standard deviations, and it has been seen that these frequencies do not provide visual comfort. On the other hand, the standard deviations of the images taken at the band level between 166, and 250 Hz light frequencies are low, and no flicker effect has been observed in the recorded photos. Therefore, the evaluation of the human vision comfort factor concluded that it would be more convenient to adjust the light PWM frequency to around the band level or above these frequencies. The key lessons learned from this study follows:

- By choosing parameters based on color metrics such as color temperature and illuminance, a balance can be achieved between light quality, and frequency in LED lighting.
- The CIE spectral sensitivity function value, and the Kruithof curve characteristics can be used to determine the human eye comfort level.

- Histogram graphs can be used effectively to determine human visual comfort.
- It has been proven that the standard deviation values in the histogram graphs of the LED light PWM frequency at values around 160 Hz and above are quite low and the light quality is quite ideal.

DISCLOSURE STATEMENT

The author declares that there are no conflicts of interest regarding the publication of this article.

REFERENCES

- [1] C. W. Lee and J. H. Kim, "Effect of LED lighting illuminance and correlated color temperature on working memory," *Int. J. Opt.*, vol. 2020, pp. 1–7, 2020. DOI: [10.1155/2020/3250364](https://doi.org/10.1155/2020/3250364).
- [2] M. A. Ozcelik, "The design and implementation of PV-based intelligent distributed sensor LED lighting in daylight exposed room environment," *Sustain. Comput. Inform. Syst.*, vol. 13, pp. 61–69, 2017. DOI: [10.1016/j.suscom.2017.01.001](https://doi.org/10.1016/j.suscom.2017.01.001).
- [3] P. Wiatr, J. Chen, P. Monti and L. Wosinska, "Energy efficiency versus reliability performance in optical backbone networks [invited]," *J. Opt. Commun. Netw.*, vol. 7, no. 3, pp. A482–A491, March 2015. DOI: [10.1364/JOCN.7.00A482](https://doi.org/10.1364/JOCN.7.00A482).
- [4] M. A. Ozcelik, "Light sensor control for energy saving in DC grid smart LED lighting system based on PV system," *J. Optoelectron. Adv. Mater.*, vol. 18, no. 5–6, pp. 468–474, 2016.
- [5] A. M. Al-Ghaili, H. Kasim, N. M. Al-Hada, M. Othman and M. A. Saleh, "A review: buildings energy savings - lighting systems performance," *IEEE Access*, vol. 8, pp. 76108–76119, 2020. DOI: [10.1109/ACCESS.2020.2989237](https://doi.org/10.1109/ACCESS.2020.2989237).
- [6] G. Shahzad, H. Yang, A. W. Ahmad and C. Lee, "Energy-efficient intelligent street lighting system using traffic-adaptive control," *IEEE Sensors J.*, vol. 16, no. 13, pp. 5397–5405, July 2016. DOI: [10.1109/JSEN.2016.2557345](https://doi.org/10.1109/JSEN.2016.2557345).
- [7] J. Byun and T. Shin, "Design and implementation of an energy-saving lighting control system considering user satisfaction," *IEEE Trans. Consum. Electron.*, vol. 64, no. 1, pp. 61–68, Feb. 2018. DOI: [10.1109/TCE.2018.2812061](https://doi.org/10.1109/TCE.2018.2812061).
- [8] Y.-L. Chang and Z.-H. Lu, "White organic light-emitting diodes for solid-state lighting," *J. Display Technol.*, vol. 9, no. 6, pp. 459–468, June 2013. DOI: [10.1109/JDT.2013.2248698](https://doi.org/10.1109/JDT.2013.2248698).
- [9] J. J. Sammarco and W. Helfrich, "Illustrating the luminaire comparison method," *IEEE Trans. Ind. Appl.*, vol. 57, no. 3, pp. 3023–3028, May–June 2021. DOI: [10.1109/TIA.2021.3057307](https://doi.org/10.1109/TIA.2021.3057307).
- [10] M. S. Shur and R. Zukauskas, "Solid-state lighting: toward superior illumination," *Proc. IEEE*, vol. 93, no. 10, pp. 1691–1703, Oct. 2005. DOI: [10.1109/JPROC.2005.853537](https://doi.org/10.1109/JPROC.2005.853537).

- [11] B.-M. Song, B. Han, A. Bar-Cohen, R. Sharma and M. Arik, "Hierarchical life prediction model for actively cooled LED-based luminaire," *IEEE Trans. Compon. Packag. Technol.*, vol. 33, no. 4, pp. 728–737, Dec. 2010. DOI: [10.1109/TCAPT.2010.2051034](https://doi.org/10.1109/TCAPT.2010.2051034).
- [12] C.-S. Wang, "Flicker-insensitive light dimmer for incandescent lamps," *IEEE Trans. Ind. Electron.*, vol. 55, no. 2, pp. 767–772, Feb. 2008. DOI: [10.1109/TIE.2007.908528](https://doi.org/10.1109/TIE.2007.908528).
- [13] J. C. W. Lam, J. C. Y. Hui and P. K. Jain, "A dimmable high power factor single-switch electronic ballast for compact fluorescent lamps with incandescent phase-cut dimmers," *IEEE Trans. Ind. Electron.*, vol. 59, no. 4, pp. 1879–1888, April 2012. DOI: [10.1109/TIE.2011.2141096](https://doi.org/10.1109/TIE.2011.2141096).
- [14] J. Gnanavadivel, N. Senthil Kumar, C. N. Naga Priya, S. T. Jaya Christa and K. S. Krishna Veni, "Single phase positive output super-lift Luo converter fed high power LED lamp with unity power factor and reduced source current harmonics," *J. Optoelectron. Adv. Mater.*, vol. 18, no. 11–12, pp. 1007–1017, 2016.
- [15] L. Svilainis, "Comparison of the EMI performance of LED PWM dimming techniques for LED video display application," *J. Display Technol.*, vol. 8, no. 3, pp. 162–165, March 2012. DOI: [10.1109/JDT.2011.2175362](https://doi.org/10.1109/JDT.2011.2175362).
- [16] S. J. Yun, Y. K. Yun and Y. S. Kim, "A low flicker TRIAC dimmable direct AC LED driver for always-on LED arrays," *IEEE Access*, vol. 8, pp. 198925–198934, 2020. DOI: [10.1109/ACCESS.2020.3034334](https://doi.org/10.1109/ACCESS.2020.3034334).
- [17] O. F. Farsakoglu and H. Y. Hasirci, "Energy optimization of low power LED drivers in indoor lighting," *J. Optoelectron. Adv. Mater.*, vol. 17, no. 5–6, pp. 816–821, 2015.
- [18] D. Rand, B. Lehman and A. Shteynberg, "Issues, models and solutions for triac modulated phase dimming of LED lamps," in Proc. IEEE Power Electron. Spec. Conf., Oct. 2007, pp. 1398–1404.
- [19] IEEE Recommended Practices for Modulating Current in High-Brightness LEDs for Mitigating Health Risks to Viewers, IEEE Standard 1789-2015, 2015. [Online]. Available: <https://standards.ieee.org/standard/1789-2015.html>
- [20] B. Lehman and A. J. Wilkins, "Designing to mitigate effects of flicker in LED lighting: reducing risks to health and safety," *IEEE Power Electron. Mag.*, vol. 1, no. 3, pp. 18–26, Sep. 2014. DOI: [10.1109/MPPEL.2014.2330442](https://doi.org/10.1109/MPPEL.2014.2330442).
- [21] C. W. Lee and J. H. Kim, "The influence of LED lighting on attention and long-term memory," *Int. J. Optics*, vol. 2020, pp. 1–6, 2020. DOI: [10.1155/2020/8652108](https://doi.org/10.1155/2020/8652108).
- [22] S. Afshari, S. Mishra, A. Julius, F. Lizarralde, J. D. Wason and J. T. Wen, "Modeling and control of color tunable lighting systems," *Energy Build.*, vol. 68, no. Part A, pp. 242–253, 2014. DOI: [10.1016/j.enbuild.2013.08.036](https://doi.org/10.1016/j.enbuild.2013.08.036).
- [23] S. Soltic and A. Chalmers, "Optimization of LED lighting for clinical settings," *J. Healthc. Eng.*, vol. 2019, pp. 5016013, 2019. DOI: [10.1155/2019/5016013](https://doi.org/10.1155/2019/5016013).
- [24] Y. Qu, W. Shu and J. S. Chang, "A low-EMI, high-reliability PWM-based dual-phase LED driver for automotive lighting," *IEEE J. Emerg. Sel. Topics Power Electron.*, vol. 6, no. 3, pp. 1179–1189, Sept. 2018. DOI: [10.1109/JESTPE.2018.2812902](https://doi.org/10.1109/JESTPE.2018.2812902).
- [25] M. Sbert, C. Ancuti, C. O. Ancuti, J. Poch, S. Chen and M. Vila, "Histogram ordering," *IEEE Access*, vol. 9, pp. 28785–28796, 2021. DOI: [10.1109/ACCESS.2021.3058577](https://doi.org/10.1109/ACCESS.2021.3058577).
- [26] P. Carbone and D. Petri, "Noise sensitivity of the ADC histogram test," IMTC/98 Conference Proceedings. IEEE Instrumentation and Measurement Technology Conference. Where Instrumentation is Going (Cat. No.98CH36222), 1998. vol. 1, pp. 88–91. DOI: [10.1109/IMTC.1998.679719](https://doi.org/10.1109/IMTC.1998.679719).
- [27] M. A. Özçelik, "The design and comparison of central and distributed light sensed smart LED lighting systems," *Int. J. Photoenergy*, vol. 2018, pp. 1–14, 2018. DOI: [10.1155/2018/4589085](https://doi.org/10.1155/2018/4589085).
- [28] "EN 12464-1, light and lighting-lighting of work places part 1: indoor workplaces," EN Standard. December 2022. <https://www.en-standard.eu/csn-en-12464-1-light-and-lighting-lightingof-work-places-part-1-indoor-work-places/>.
- [29] I. Chew, V. Kalavally, N. W. Oo and J. Parkkinen, "Design of an energy-saving controller for an intelligent LED lighting system," *Energy Build.*, vol. 120, pp. 1–9, 2016. DOI: [10.1016/j.enbuild.2016.03.041](https://doi.org/10.1016/j.enbuild.2016.03.041).

BIOGRAPHIES

Mehmet Ali Ozcelik (Senior Member IEEE) received B.S., M.S., and PhD Degrees in Electrical Education/Electrical and Electronics Engineering from Marmara University/Harran University, Istanbul/Şanlıurfa and Electrical & Electronics Engineering, Kahramanmaraş Sutcu Imam University, Turkey, in 1999, 2006, and 2015 respectively. He has been in Center for Future Energy Systems at the Rensselaer Polytechnic Institute, New York as a visiting/post-doc researcher from 2018 to 2020. He is currently an Assoc. Prof. Dr. at the Department of Electric and Energy, Gaziantep University, Turkey. His field of interest includes Renewable energy, and electrical power systems, Micro grids, and Smart lighting systems.

Tahir Cetin Akinci (Senior Member IEEE) pursued his Bachelor's degree in Electrical Engineering in 2000, followed by his Master's and Ph.D. degrees in 2005 and 2010, respectively. From 2003 to 2010, he worked as a Research Assistant at Marmara University in Istanbul, Turkey. Dr. Akinci is currently a full professor in the Electrical Engineering Department at Istanbul Technical University (ITU) in 2020. Dr. Akinci assumed the role of a visiting scholar at the University of California Riverside (UCR). His research interests include power systems, artificial neural networks, deep learning, machine learning, cognitive systems, signal processing, and data analysis.

Musa Yilmaz (Senior Member, IEEE) received the B.S., M.S., and Ph.D. degrees in electrical and electronics

engineering, in 2001, 2004, and 2013, respectively. From 2004 to 2014, he was with Dicle University, Diyarbakır, Turkey. Since 2014, he has been an Assistant Professor with the Electrical and Electronics Engineering Department, Batman University. In 2015 and 2016, he was a Visiting Scholar with the University of California at Los Angeles (UCLA). Since 2022, he has been a Visiting Scholar with the University of California at Riverside (UCR). He is currently a Partner with Biosys LLC. His research interests include smart grids, renewable energy, power systems, artificial neural networks, deep learning, machine learning, signal processing, and data analysis. Dr. Yılmaz served as the Editor-in-Chief for the Balkan Journal of Electrical and Computer Engineering (BAJECE) and the European Journal of Technique (EJT).

Alfredo A. Martinez-Morales is the Managing Director of the Southern California Research Initiative for Solar Energy (SC-RISE) and Research Professor at the Bourns College of Engineering Center for Environmental Research and Technology (CE-CERT). Dr. Martinez-Morales received his Ph.D., M.S. and B.S. degrees in electrical engineering from University of California Riverside (UCR). His current research includes solar cells, alkali metalion batteries, highly integrated renewables, energy storage systems, and micro grids. Dr. Martinez-Morales is a principal investigator in the Sustainable Integrated Grid Initiative (SIGI) at UCR, and has contributed in the engineering, permitting, and deployment of the SIGI smart grid testbed system and multiple micro grids throughout Southern California.